



HAL
open science

Mapping of quadrature magnetic susceptibility/magnetic viscosity of soils by using multi-frequency EMI

François-Xavier Simon, Apostolos Sarris, Julien Thiesson, Alain Tabbagh

► To cite this version:

François-Xavier Simon, Apostolos Sarris, Julien Thiesson, Alain Tabbagh. Mapping of quadrature magnetic susceptibility/magnetic viscosity of soils by using multi-frequency EMI. *Journal of Applied Geophysics*, 2015, 120, pp.36-47. 10.1016/j.jappgeo.2015.06.007 . hal-01376254

HAL Id: hal-01376254

<https://hal.sorbonne-universite.fr/hal-01376254>

Submitted on 4 Oct 2016

HAL is a multi-disciplinary open access archive for the deposit and dissemination of scientific research documents, whether they are published or not. The documents may come from teaching and research institutions in France or abroad, or from public or private research centers.

L'archive ouverte pluridisciplinaire **HAL**, est destinée au dépôt et à la diffusion de documents scientifiques de niveau recherche, publiés ou non, émanant des établissements d'enseignement et de recherche français ou étrangers, des laboratoires publics ou privés.

1 **Mapping of quadrature magnetic susceptibility/magnetic viscosity of soils by using**
2 **multi-frequency EMI**

3

4 François-Xavier Simon¹, Apostolos Sarris¹, Julien Thiesson², Alain Tabbagh²

5

6 ¹ Lab GeoSat ReSeArch, IMS-FORTH, Rethymno

7 ² Sorbonne Universités, UPMC –Paris6, UMR7619-Métis, F-75252, Paris

8

9 **Abstract**

10 Measuring magnetic viscosity significantly improves the information brought by the
11 magnetic susceptibility about the history of soils. In the field its mapping can be achieved by
12 TDEM measurement. Here we study the applicability of multi-frequency FDEM viscosity
13 measurement in the low frequency range using a commercial EMI instrument. The
14 dependence of the in-phase and quadrature out-of-phase components of the ratio of secondary
15 magnetic field to primary magnetic field, electrical conductivity, magnetic susceptibility and
16 magnetic viscosity is first described. The procedure allowing the determination of the three
17 apparent properties is then proposed. It delivers first the conductivity using the differences
18 between the quadrature responses at two different frequencies. Then, after removing the
19 conductivity effects both in the in-phase and quadrature components, it provides the values of
20 the magnetic susceptibility and viscosity. This procedure is tested on 1D and 3D synthetic
21 cases to assess any arising uncertainty. The application of the method is attested in two
22 archaeological case histories in Thessaly in conductive and magnetic soil contexts. The
23 apparent magnetic viscosity maps are significantly different from magnetic susceptibility and
24 conductivity maps thus bringing new information into the game.

25

26 **Keywords**

27 Low induction number, EMI, soil magnetic viscosity, soil magnetic susceptibility, soil
28 electrical conductivity, multi-frequency.

29

30 **Introduction**

31 Frequency domain electromagnetic induction (EMI) instrument with Slingram
32 geometry (dipole-dipole) is of common use in archaeological prospection (Scollar *et al.*,
33 1990) and soil studies (Corwin and Lesch, 2005). It allows mapping simultaneously electrical
34 conductivity and magnetic susceptibility of soils. These light mobile instruments present also
35 the advantage to be easily towed on the field (De Smedt *et al.*, 2013).

36 For the low frequency domain, the choice to neglect displacement currents limits the
37 used frequencies to 100 kHz and the geometric scale of the instruments, i.e. the metric inter-
38 coil separation, determines the investigated volume. Consequently these EMI instruments
39 respect the low induction number (LIN) approximation and thus: (1) the conductivity
40 response is in quadrature out-of-phase from the transmitter moment that allows the
41 measurement of the in-phase magnetic susceptibility, (2) the depth of investigation is only
42 governed by the instrument's geometry. Only geometrical soundings can be achieved;
43 therefore there is no advantage in using different frequencies.

44 Until now, with EMI frequency domain instruments, only the in-phase magnetic
45 susceptibility is measured, while quadrature susceptibility/magnetic viscosity has been
46 measured and mapped using TDEM instruments (Thiesson *et al.* 2007). However, some
47 observations of this property with single frequency instruments have been also achieved (Mc
48 Neill 2013).

49 To improve the interpretation of FDEM measurements one faces a series of
50 difficulties; on one hand the magnetic susceptibility is a complex quantity which generates a

51 quadrature response that algebraically adds to the conductivity response and, on the other
52 hand, the LIN approximation and low frequency approximation have their own limits. When
53 either the conductivity or the frequency increases, a significant in-phase response appears that
54 algebraically adds to the in-phase susceptibility response. Over clayed soils, the dielectric
55 permittivity can also be sufficiently high to generate measurable responses in the higher
56 portion of the low frequency range.

57 The use of several frequencies has been considered to overcome these limitations.
58 Limiting the purpose of the present paper to magnetic properties, it is first preferable to stay in
59 the lower part of the frequency range around or below 10 kHz. In this range, due to the
60 absence of frequency dependence of the quadrature component of soil magnetic susceptibility
61 (Mullins and Tite 1973), it is possible to separate its response from the one generated by the
62 conductivity, which increases with frequency. This solution has already been proposed
63 (Tabbagh, 1986a) and a two-frequency prototype instrumentation has been tested (Benech,
64 2000).

65 Since 1996, a multi-frequency commercial instrument, the GEM-2, has become
66 available. Its manufacturers claimed that it allows frequency soundings (Won et al., 1996).
67 This statement raised a contestation (Mc Neill, 1996) recalling the LIN approximation
68 implications. The argument was closed by the admission (Huang and Won, 2003) that
69 frequency soundings can only be relevant for higher induction number conditions when the
70 ground conductivity is sufficiently high (sea water bathymetry). Nevertheless, it remains
71 interesting to check the results that can be obtained in practice with such multifrequency
72 instrument for both electrical conductivity and complex magnetic susceptibility. In particular,
73 the TDEM measurements, used to map of the quadrature susceptibility/magnetic viscosity,
74 indicated spatial variations that can be significantly different from those of the magnetic

75 susceptibility and can be more clearly linked with nitrogen or carbon content of a soil
76 (Thiesson *et al.*, 2012).

77 In the present paper, after a short recall about the soil electromagnetic properties and
78 the theoretical responses they generate, we will consider synthetic and experimental results
79 obtained in different sites and discuss about the reliability of quadrature susceptibility
80 mapping.

81

82 **Measured soil properties**

83 In the frequency range where the displacement currents proved to be neglected (below
84 100 kHz), the electrical resistivity, ρ , is well defined and extends from 1 to 2 $\Omega\cdot\text{m}$ in the
85 intertidal zone to 10000 $\Omega\cdot\text{m}$ in permafrost or in crystalline dry soils. This very wide dynamic
86 range is the greatest observed for usual geophysical properties, but values out of the [10, 1000
87 $\Omega\cdot\text{m}$] interval remain occasional in soils studies. In accordance with the hypothesis where the
88 polarization effects are negligible, in the particular range the conductivity is assumed
89 independent of the frequency.

90 On the contrary, the magnetic susceptibility is complex and varies with frequency
91 (Mullins, 1977); it must thus be written: $\kappa(\omega) = \kappa_{ph}(\omega) - i\kappa_{qu}(\omega)$ where ω is the angular
92 frequency, κ_{ph} is the in-phase component and κ_{qu} the quadrature component. However, all the
93 experiments, except those from iron working sites, undertaken over laboratory samples
94 respect the dispersed single-domain grain theory (Néel, 1949) which states that the quadrature
95 component is constant and linked to the frequency variation of the in-phase part by::

$$96 \quad \frac{2}{\pi} \kappa_{qu} = - \frac{\partial \kappa_{ph}(\omega)}{\partial \ln(\omega)} \quad (1)$$

97 (Mullins and Tite 1973, Dabas *et al.* 1992, Dabas and Skinner 1993). This decrease of the in-
98 phase susceptibility and the value of the quadrature susceptibility correspond to the same
99 parameter called magnetic viscosity. The viscosity is also measured in the field using TDEM
100 instruments (Colani and Aitken 1966, Thiesson *et al.* 2007) and all the field results, (see for
101 example Pétronille *et al.* 2010), correspond to a slope of the logarithmic decrease close to -1
102 for the $\frac{\partial B(t)}{\partial t}$ signal measured in the receiver coil in accordance with the above formula. The
103 in-phase soil susceptibility range of values is also quite large, from $1000 \cdot 10^{-5}$ SI in volcanic
104 areas to $10 \cdot 10^{-5}$ SI, but values close to $1000 \cdot 10^{-5}$ SI are rare. Due to the presence of small
105 mono-domain/superparamagnetic grains the quadrature susceptibility is significant and more
106 often of the order of 6% of the in-phase susceptibility.

107 Consequently we will interpret the soil responses to a low frequency field excitation
108 by considering a constant conductivity and a susceptibility following equation (1). The
109 calculation of the response of a homogeneous ground, or of layered one, has been established
110 by the work of Wait (1959), and is based on Hankel's transforms that can be rapidly
111 calculated using convolution products (Guptasarma and Singh, 1997). Complete expressions
112 and a description of the different subsequent approximations can be found in (Thiesson *et al.*
113 2014). They allow expressing the measurement in terms of apparent conductivity and
114 apparent susceptibility, based on a simplified conversion since the variations are monotonous
115 although not simply linear.

116 To simplify the expressions in the following parts of the text, one will use the term
117 magnetic susceptibility for the in-phase part only and use the term magnetic viscosity for the
118 quadrature out-of-phase part.

119

120 GEM-2 instrument specificity

121 In this study we process data acquired with the GEM-2 instrument (Figure 1). This
122 multi-frequency instrument is not a simple coplanar coil configuration Slingram device, but
123 instead it has in fact two receivers coils, one serving as bucking coil for the other (Won *et al.*
124 1996). They have the same surface and are mounted in opposite directions in such way that
125 the primary field is exactly compensated: the “bucking” coil at a 1.035m distance from the
126 transmitter coil having four times less turns than the “receiver” located at 1.66m distance. The
127 measured quantity is thus: $\frac{(H_{sR} - H_{sB} / 4)}{H_p}$, where H_p is being the primary field at the
128 ‘receiver’ location, H_{sR} the secondary field at the ‘receiver’ location and H_{sB} the secondary
129 field at the ‘bucking’ location. Thus, one must first reconsider the relationships between this
130 measured quantity and the ground properties.

131 Figure 2 presents the responses for both conductivity and in-phase susceptibility (the
132 quadrature susceptibility being 6% of the in-phase) at 5 kHz and 40 kHz for the characteristics
133 of the GEM-2 instrument when held at 0.3m height above the ground surface. It can be
134 observed that while the quadrature response is simply correlated (quasi proportional) with the
135 ground conductivity, the in-phase sensitivity to susceptibility changes is hampered by the in-
136 phase conductivity response which seems totally dominating the response for lower
137 susceptibilities at 40 kHz.

138 Another important aspect is the dependence on the height above the ground, as the
139 HCP configuration is known to exhibit changes from positive to negative values in the in-
140 phase response when the altitude increases (Tabbagh, 1986a). Figure 3 shows that while the
141 quadrature response monotonically decreases with the altitude H, the in-phase one exhibits a
142 sharp maximum around H=0.3 m. This response is shifted towards negative values when the

143 conductivity increases but it retains the same shape. This effect of the HCP configuration
144 considerably affects the shape and the sign of the anomaly for the apparent magnetic
145 susceptibility as its vertical distribution varies due to the pedogenesis process and sedimentary
146 disturbance.

147 As can be observed in Figure 4 the response generated by the quadrature susceptibility
148 is linear but of quite limited magnitude compared to the electrical conductivity response. This
149 effect explains the invisibility of the magnetic viscosity on the raw data which more often
150 appear only related to the electrical conductivity.

151

152 **Methodology**

153 The aim of any type of geophysical prospection is to identify the physical properties
154 and the geometrical shapes of the different media present in the underground. This is achieved
155 through a full inversion process but before implementing this heavy process, and to be able to
156 start it with a relevant guess of a priori parameter values, it is necessary to have a first
157 assessment of the information by transforming the raw data to apparent property variations.
158 The general definition of an apparent property is the one of a homogeneous ground that would
159 deliver the same measurement with the same instrument. Establishing apparent electrical
160 conductivity, susceptibility and viscosity maps is the purpose of the present work but as
161 several properties intervene the task is more difficult than when only one property can be
162 considered, as is the case in D.C. resistivity prospecting where the transformation corresponds
163 to a simple multiplication by a coefficient. Thus, it is necessary to describe the successive
164 steps of the transformation of the raw data in apparent properties because different procedures
165 would lead to (slightly but certainly) different results.

166 Measurement first implies a calibration step, e.g. transformation of instrumental digits
167 into experimental (Hs/Hp) ratio in ppm, established on a methodology described by Thiesson
168 *et al.* 2014). For the quadrature channel it is based on a comparison between an electrical
169 sounding and measurements at (at least) two heights above the ground surface. In this case,
170 we assume that the higher measurement is almost not affected by the magnetic properties but
171 only by electrical conductivity. Thus, one obtains the calibration coefficient between the
172 digits measured by the instrument and the theoretical response for the quadrature part of the
173 EM signal. In the second calibration step the experimental in-phase response acquired with an
174 aluminum sphere is compared with the theoretical one (Thiesson *et al.* 2014). For our
175 instrument, in-phase coefficient is -0.70 digit/ppm and the quadrature coefficient -1.0
176 digit/ppm. We repeat this calibration at each different field of survey, to ensure the stability of
177 the instrument.

178 To extract apparent complex magnetic susceptibility it's required to beforehand
179 calculate the electrical conductivity. Multi-frequency measurements allow removing the effect
180 of the magnetic viscosity on the quadrature part of the signal. Considering the difference
181 between two different frequencies this difference is then transformed in apparent electrical
182 conductivity by correspondence with a reference curve calculated using the complete
183 formulas (Thiesson *et al.* 2014).

184 In the second step of the procedure, the conductivity value is used to calculate the in-
185 phase and quadrature parts of the signal generated by the electrical conductivity at each
186 frequency. By subtracting these parts from the experimental data one can remove the
187 conductivity parts on both in-phase and quadrature channels and retain the parts generated by
188 the susceptibility and the viscosity. Magnetic viscosity strictly affects quadrature out-of-phase
189 part of the EM signal while the magnetic susceptibility only affects the in-phase part of the
190 signal. These imaginary and real parts of the secondary to primary field ratio, in ppm, are then

191 expressed in the apparent properties by comparing the values with master curves (magnetic
192 susceptibility as a function of in-phase part of the EM signal in ppm, and magnetic viscosity
193 as a function of quadrature out-of-phase part of the EM signal in ppm). The master curves
194 were beforehand calculated using the full analytical solution.

195

196 **Synthetic data**

197 The advantages of synthetic data processing is to evidence the difficulties that can
198 exist in the process before any perturbations generated during field work, the introduction of
199 external noise and possible instrument default or failure(s). Synthetic data will be analyzed
200 through a 1D case and a simple 3D geometry case.

201 *1D synthetic data*

202 As the raw data transformation applied to homogeneous ground responses restitutes
203 the exact values of the three properties one considers here a two layers model. The first layer
204 ($\rho=100 \Omega.m$, $\kappa_{phf1}=100.10^{-5}$ SI, $\kappa_{phf2}=95.6.10^{-5}$ SI, $\kappa_{qu}=6.10^{-5}$ SI) has an increasing thickness,
205 starting to 0.1 meter up to 3 meter, the second one is a more conductive and less magnetic
206 ($\rho=50 \Omega.m$, $\kappa_{phf1}=10.10^{-5}$ SI, $\kappa_{phf2}=9.56.10^{-5}$ SI, $\kappa_{qu}=0.6.10^{-5}$ SI). The susceptibility variation
207 with frequency respects equation (1) for the frequencies of 5010 and 13370 Hz used by GEM-
208 2. We simulated the response for the GEM-2 in a HCP configuration, at 0.3 m elevation. The
209 variation of the apparent susceptibility is shown in Figure 5a and that of the apparent viscosity
210 in Figure 5b. We observe a slight influence of the frequency that increases with the thickness
211 of the first layer; it is low but clearly observable for the viscosity due to the small values of it.
212 This corresponds to the apparent conductivity change, even if not totally corrected in the two
213 layer case by the applied procedure: the slope of the quadrature response against viscosity is
214 slightly dependent on the conductivity. The apparent magnetic viscosity delivered by the used

215 procedure is thus in (small) dependence on the electrical conductivity as shown in Figure 6 for
216 both 5010 and 13370 frequencies. In this Figure the absence of conductivity dependence
217 would correspond to horizontal straight lines for each magnetic viscosity value, and globally
218 one can observe that its dependence is low. However, one must notice that the discrepancy (1)
219 increases with frequency, (2) is, as expected, high for smaller viscosity values, but (3)
220 increases also for high resistivity. In this last case the uncertainty is generated by the
221 uncertainty in the evaluation of the resistivity itself.

222 Finally this example underlines that the determination of an apparent magnetic
223 viscosity value using the proposed procedure is still valuable for medium and high magnetic
224 viscosity (still as a possible value for common soil). As the discrepancy is frequency
225 dependent, the determination of the magnetic viscosity with the lowest frequencies is much
226 more preferable.

227 *3D synthetic data*

228 3D synthetic data were simulated by the moment method (Tabbagh, 1985). We put a
229 resistive and magnetic block ($\rho=500 \Omega\text{m}$, $\kappa_{\text{phf1}}=150.10^{-5} \text{ SI}$, $\kappa_{\text{phf2}}=143.10^{-5} \text{ SI}$, $\kappa_{\text{qu}}=10.10^{-5} \text{ SI}$)
230 in a two layers medium. The first layer, of 0.2 m thickness, is more resistive and magnetic
231 ($\rho=100 \Omega\text{m}$, $\kappa_{\text{phf1}}=50.10^{-5} \text{ SI}$, $\kappa_{\text{phf2}}=49.10^{-5} \text{ SI}$, $\kappa_{\text{qu}}=3.10^{-5} \text{ SI}$) than the second one ($\rho=50 \Omega\text{m}$,
232 $\kappa_{\text{phf1}}=10.10^{-5} \text{ SI}$, $\kappa_{\text{phf2}}=9.10^{-5} \text{ SI}$, $\kappa_{\text{qu}}=1.10^{-5} \text{ SI}$) as we have usually noticed on well-drained
233 soil. In accordance with the Neel's theory the in-phase magnetic susceptibility still decreases
234 with the frequency, depending on the value of the magnetic viscosity. The target is a block of
235 $2 \times 2 \times 2 \text{ m}^3$ centered at a depth of 1.2 m, i.e. entirely in the second layer. The top of this
236 target is close to the ground surface. This simulation uses the same acquisition parameters as
237 in-field acquisition: a 1m measurement step, an altitude of 0.3 meter in the HCP configuration
238 and with the same instrumental settings. We again used the two first frequencies of the

239 instrument, 5010 Hz and 13370 Hz. The synthetic data are then processed with the previously
240 introduced procedure. We obtain 5 maps (Fig. 7): electrical conductivity on the one hand,
241 magnetic susceptibility and magnetic viscosity at both frequencies on the other hand.

242 As expected from previous theoretical studies (Tabbagh 1986b) for HCP
243 configuration, the apparent electrical conductivity shows a complex shaped anomaly, which
244 even for such a simple shaped target has three extrema. The shape of the apparent magnetic
245 susceptibility contours is simpler than the electrical one. It shows a high value just above the
246 center of the target and weak negative values around the block, but the shape of the anomaly
247 and the shape of the target present differences. This point needs to be taken into account in the
248 further interpretation steps. Considering the frequencies, both maps are exactly similar. For
249 both frequencies the modes of apparent in-phase (susceptibility) and quadrature (viscosity)
250 values are governed by the instrument geometry and without link with the anomalous
251 causative body. We thus consider the variation of the data expressed by the difference
252 between the maximum and minimum values of the anomaly on each map. At 5010 Hz
253 frequency the differences are $204 \cdot 10^{-5}$ SI in-phase and $15.3 \cdot 10^{-5}$ SI in quadrature. This
254 corresponds to a ratio of 7.5% between the two components. At 13370 Hz frequency the
255 corresponding values are $184.9 \cdot 10^{-5}$ SI, 15.510^{-5} SI and 8.4%. The amplitude of the in-phase
256 susceptibility slightly decreases with frequency while the quadrature (viscosity) practically
257 remains constant (considering the error resulting from the non-strictly addition of magnetic
258 viscosity and electrical conductivity) in agreement with the susceptibility values introduced in
259 the modelling. The viscosity/susceptibility ratio is slightly higher than the ratio of the body
260 properties (6.7%) but this can also be explained by the influence of the higher ratio chosen for
261 the second layer (11.1%).

262

263 **Field tests**

264 We employed the GEM-2 in two archaeological sites to map the complex magnetic
265 susceptibility and the electrical conductivity. These two sites are located on the Thessaly plain
266 in central Greece. The first one, Karatzantakli, in the mountain area, is covered by a high clay
267 content soil which suggests a high conductivity. The second one, Almiriotiki, in plain, close
268 to paleo-channel and floodplain deposits has also high clay content but with strong
269 heterogeneities affecting the electrical conductivity. These human settlements are likely to
270 change magnetic properties of soils and generate anomalies related to the archaeological
271 features and handcraft activities area. It also looks well-suited to our studies. In-phase parts of
272 the signal are affected by the electrical conductivity. As showed on the methodological part,
273 the use of different frequencies allows removing its first order in-phase and quadrature
274 effects. We are thus able to map the magnetic viscosity distribution over the area cover by the
275 EM data and observe its significance.

276 Five different frequencies from 5010 Hz until 40050Hz (5010 Hz, 13370 Hz, 22530
277 Hz 31290Hz and 40050 Hz) were used. Measurements were continuously acquired almost
278 every meter along profiles 1m apart. The instrument was carried at an altitude of 0.3 m above
279 the ground surface. Despite manufacturer advice, we preferred to carry the instrument at this
280 height regarding the curve of sensitivity for the magnetic properties on the in-phase part of the
281 instrument. Only the two lower frequencies are considered here for magnetic properties
282 mapping.

283 ***Karatzantakli***

284 Karatzantakli is a Neolithic tell (“magoula”), consisting of an accumulation of
285 anthropogenic material, which means high soil heterogeneity. On this site geomorphological
286 variations are induced by different cover material in the different parts of the site. Some

287 features like kilns or fireplaces could increase considerably the magnetic susceptibility or the
288 magnetic viscosity at some points. Measurements were recorded in a manual mode.
289 Measurements were automatically acquired along the profile with a regular distribution of the
290 measurements along each one.

291 The raw data, in Figure 8, show high contrast on the quadrature part of the signal and
292 on the in-phase part of the EM signal. For the in-phase part of the signal, ranges of values are
293 similar at both frequency but with a marked offset. On the quadrature out-of-phase part of the
294 signal, the range of values for the higher frequency is approximately two times higher than for
295 the lower frequency and both show a high conductivity who do affect the in-phase part of the
296 EM signal (Fig. 8).

297 The five maps resulting from the raw data processing are presented in Figure 9.
298 Apparent electrical conductivity shows some differences between the left and right parts of
299 the area.. The important depth of investigation for this instrument in HCP geometry doesn't
300 allow any shallow characterization of the soils and it is more representative of a too thick
301 layer of soil. Apparent magnetic susceptibility shows more anomalies on the whole area.
302 Values of susceptibility are extremely high. For 5010 Hz the median of values is 227.10^{-5} SI
303 and the interquartile is 73.10^{-5} . These values of magnetic susceptibility correspond with very
304 high values of magnetic viscosity due to the inter dependence of magnetic susceptibility and
305 magnetic viscosity. The inter-quartile difference changes from 73.10^{-5} SI to 71.10^{-5} between
306 the two frequencies. Decreasing of interquartile seems very small regarding the high value of
307 magnetic susceptibility but could be also an effect of the distribution of the magnetic
308 susceptibility. Some anomalies are common on both magnetic susceptibility and magnetic
309 viscosity but generally speaking the maps look quite different. This means that the ratio of
310 magnetic viscosity on magnetic susceptibility is varying from on part to another one which
311 implies different compositions regarding the size of the magnetic grains. These differences

312 confirm the interest to be attentive to this soil property regarding the EM signal. The range of
313 values of the ratio between magnetic viscosity interquartile value and magnetic susceptibility
314 interquartile value is close to 26%. This high value could probably be explained by an
315 insufficiently good relative gain calibration between the in-phase and quadrature channels.

316 *Almiriotiki*

317 The second field test is the Neolithic tell of Almiriotiki. Measurements were acquired
318 with a GPS RTK (Javad Triumph) which allows covering a very large area in one day (around
319 2 ha/day). Accuracy of the positioning is better than decimetric due to the differential
320 correction of the GPS point. This site presents a settlement covering the top part of the tell
321 (magoules) and a bottom part around the central elevation.

322 We present the raw data for the in-phase part and the quadrature parts of the EM signal
323 in Figure 10. For the in-phase part we observe an offset between the two frequencies but the
324 same dynamic range of values. Only small differences can be attributed to the electrical
325 conductivity, especially in the north part of the map. The quadrature part of the signal shows
326 two similar maps for the both frequencies, with contrasted ranges of values. This frequency
327 evolution is the consequence of the dependence on the frequency of the electrical conductivity
328 measurements. Both frequency and dynamic range of values are approximately multiplied by
329 a factor of two. At first glance the part of magnetic properties is invisible on both quadrature
330 and in-phase response maps.

331 The processing allows us to obtain the five different maps presented in Figure 11. In
332 appearance, electrical conductivity is very close to the raw data due to the strong effect of the
333 electrical conductivity on the quadrature part of the signal. The values of the conductivity
334 show a global high conductivity. On the north part, the conductivity increases, probably due
335 to the soil modification induced by flooding deposits. It explains the effect of the conductivity

336 on the in-phase part of the raw data for the same location. The tell is more resistive due to the
337 mix of anthropogenic material and natural clay soils. For the susceptibility, interpretation is
338 less obvious which is not surprising regarding the HCP configuration.

339 Both magnetic viscosity maps are very similar. In this case data are noisier than in
340 previous example. Nevertheless value of magnetic susceptibility between 100 and $300 \cdot 10^{-5}$
341 S.I. is still very high. Regarding the link between the magnetic susceptibility and the magnetic
342 viscosity we can again expected high value of magnetic viscosity. Ratio of magnetic
343 susceptibility and magnetic viscosity (inter-quartiles) is still higher than expected and close to
344 22%. Again, this effect could be derived from a poor calibration but again the viscosity maps,
345 very coherent between the two frequencies, show underground patterns significantly different
346 from those shown by susceptibility maps. This again demonstrates the high interest of
347 viscosity measurements.

348

349 **Discussion**

350 The experiments here presented were acquired using the GEM-2 instrument in HCP
351 configuration. This configuration and the existence of two receivers do not facilitated the
352 interpretation but this manufacturer's design implies a better stability when moving the
353 instrument on the field. In near future, it is necessary to implement the use of VCP geometry
354 by improving the stability of the instrument and correcting for the slight modification of the
355 axis orientation during a continuous acquisition. Regarding the greater simplicity of VCP
356 sensitivity curves, these improvements will allow a better description of the magnetic
357 viscosity underground variations. However, in its present configuration the GEM-2 is already
358 usable to perform a significant and qualitatively reliable magnetic viscosity mapping at the
359 same time as conductivity and magnetic susceptibility mappings.

360 Due to the different physical properties taken into account, the transformation of the
361 raw data in apparent properties is not straightforward but it is efficient. If the quantitative
362 interpretation must use the raw data, the mapping of apparent properties proves to be feasible
363 and informative. As the way to express the apparent properties is clearly established and the
364 uncertainty assessed, it is possible to take into account the potential error on the estimation.
365 The adopted definition of the apparent properties is thus satisfactory; especially because the
366 error effect of this assumption is lower than the spatial variability of soil properties.
367 Nevertheless, this error adds to the possible different gains between the in-phase and
368 quadrature measurement channels, and prevents any precise quantitative determination of the
369 ratio between the magnetic susceptibility and the magnetic viscosity, which can open the way
370 to study the in-field variations of the grain size distributions. In all published magnetic
371 viscosity measurements in the field (Thiesson *et al.* 2007, Pétronille *et al.* 2010), the maps of
372 this ratio were informative and from the archaeological point of view supported assumptions
373 about the functions of the detected features (metallurgy, pottery, domestic waste). In paleo-
374 soil studies too, when this ratio is recalculated from the frequency dependence of the in-phase
375 magnetic susceptibility, this ratio is more discriminant for layer identification than the
376 susceptibility itself (Thiesson 2007)

377

378 **Conclusion**

379 The first series of tests and experiments aiming at mapping the magnetic viscosity,
380 together with the electrical conductivity and the magnetic susceptibility, using a commercial
381 multi-frequency FDEM instrument have been demonstrated. In spite that the instrument
382 characteristics and its coil configuration are far from optimal for soil studies, the results are
383 convincing and the experiments confirm its effectiveness in mapping this parameter: the

384 viscosity maps are not simple traces of the in-phase component of the magnetic susceptibility.
385 Further comparisons with TDEM measurements are planned to elucidate the relative
386 advantages of both ways of measurement. For FDEM, going ahead in the study of the
387 magnetic grain sizes distribution necessitates to adopt a more convenient coil configuration
388 and to progress in the relative gain calibration between in-phase and out-of-phase channels.

389 In the two examples examined, only the two lower frequencies were taken into
390 account. For these frequencies the proportionality of the quadrature response with the
391 conductivity is almost exact and only in high conductivity areas the effect on the in-phase part
392 of the signal can be observed. When increasing the frequency, another parameter may affect
393 the responses, namely the dielectric permittivity (Huang and Fraser, 2001). A significant
394 amount of work must yet to be undertaken to assess all the possibilities offered by low
395 frequency EMI instruments in soil study contexts.

396

397 **Acknowledgments**

398 This work was performed in the framework of the IGEAN (“Innovative Geophysical
399 Approaches for the study of Early Agricultural villages of Neolithic”) project which is
400 implemented under the "ARISTEIA" Action of the "OPERATIONAL PROGRAMME
401 EDUCATION AND LIFELONG LEARNING" and is co-funded by the European Social
402 Fund (ESF) and National Resources.

403

404 **References**

- 405 Benech, C., 2000. Interprétation conjointe de cartographies magnétique et électromagnétique
406 des propriétés magnétiques des sols anthropisés. UPMC, Paris.
- 407 Colani, C., Aitken, M.J., 1966. A new type of locating device. I field trials. *Archaeometry*, **9**,
408 9–19.
- 409 Corwin, D.L., Lesch, S.M., 2005. Characterizing soil spatial variability with apparent soil
410 electrical conductivity: I. survey protocols. *Computers and Electronics in Agriculture*,
411 46, 103-133.
- 412 Dabas, M., Jolivet, A., Tabbagh, A., 1992. Magnetic susceptibility and viscosity of soils in a
413 weak time varying field. *Geophysical Journal International*, **108**, 101–109.
- 414 Dabas, M., Skinner, J., 1993. Time-domain magnetization of soils (VRM), experimental
415 relationship to quadrature susceptibility. *Geophysics*, **58**, 326–333.
- 416 De Smedt, P., Saey, T., Lehouck, A., Stichelbaut, B., Meerschman, E., Islam, M.M., van
417 DeVijver, E., van Meirvenne, M., 2013. Exploring the potential of multi-receiver EMI
418 survey for geoarchaeological prospection: A 90 ha dataset. *Geoderma*, **199**, 30-36.
- 419 Guptasarma, D., Singh, B., 1997. New digital linear filters for Hankel J0 and J1 transforms.
420 *Geophysical Prospecting*, **45**, 745–762.
- 421 Huang, H., Fraser, D., 2001. Mapping of the resistivity, susceptibility, and permittivity of the
422 earth using a helicopter-borne electromagnetic system. *Geophysics*, **66**, 148–157.
- 423 Huang, H., Won, I., 2003. Real-time resistivity sounding using a hand-held broadband
424 electromagnetic sensor. *Geophysics*, **68**, 1224–1231.
- 425 Mc Neill, J.D., 1996. Why doesn't Geonics limited build a multi-frequency EM31 or EM38?
426 *Technical note TN-30*, Geonics ltd, 5p.
- 427 Mc Neill, 2013. The magnetic susceptibility of soils is definitely complex. *Technical note TN-*
428 *36*, Geonics ltd, 27p.

429 Mullins, C.E., 1977. Magnetic susceptibility of the soil and its significance in soil science – a
430 review. *Journal of Soil Science*, **28**, 223–246.

431 Mullins, C.E., Tite, M.S., 1973. Magnetic viscosity, quadrature susceptibility, and frequency
432 dependence of susceptibility in single-domain assemblies of magnetite and
433 maghemite. *Journal of Geophysical Research*. **78**, 804–809.

434 Néel, L., 1949. Théorie du traînage magnétique des ferromagnétiques en grains fins avec
435 application aux terres cuites. *Annales de Géophysique*, **5**, 99–136.

436 Pétronille, M., Thiesson, J., Simon, F.-X., Buchsenschutz, O., 2010. Magnetic signal
437 prospecting using multiparameter measurements: the case study of the Gallic Site of
438 Levroux. *Archaeological Prospection*, **17**, 141–150.

439 Scollar, I., Tabbagh, A., Herzog, I., Hesse, A., 1990. Archaeological prospecting and remote
440 sensing, Cambridge University Press.

441 Tabbagh, A., 1985. The response of a three-dimensional magnetic and conductive body in
442 shallow depth electromagnetic prospecting. *Geophysical Journal of the Royal
443 Astronomical Society* **81**, 215–230.

444 Tabbagh, A., 1986a. Applications and advantages of the Slingram electromagnetic method for
445 archaeological prospecting. *Geophysics*, **51**, 576–584.

446 Tabbagh, A., 1986b. What is the best coil orientation in the slingram electromagnetic
447 prospecting method?, *Archaeometry*, **28**, 185–196.

448 Thiesson, J., Boulonne, L., Buvat, S., Jolivet, C., Ortolland, B., Saby, N., 2012. Magnetic
449 properties of the French soil monitoring network: first results. Near Surface
450 Geoscience 2012 - 18th European Meeting of Environmental and Engineering
451 Geophysics, EAGE.

452 Thiesson, J., Kessouri, P., Schamper, C., Tabbagh, A., 2014. Calibration of frequency-domain
453 electromagnetic devices used in near-surface surveying. *Near Surface Geophysics*, **12**,
454 481-491.

455 Thiesson J; 2007. Mesure et cartographie de la viscosité magnétique des sols. *PhD thesis*,
456 UPMC university, Parirs.

457 Thiesson, J., Tabbagh, A., Flageul, S., 2007. TDEM magnetic viscosity prospecting using a
458 Slingram coil configuration. *Near Surface Geophysics*, **5**, 363–374.

459 Wait, J., 1959. Induction by an oscillating magnetic dipole over a two layer ground. *Applied*.
460 *Science Research*, **B 7**, 73–80.

461 Won, I., Keiswetter, D., Fields, G., Sutton, L., 1996. GEM-2: A New Multifrequency
462 Electromagnetic Sensor. *Journal of Environmental and. Engineering Geophysics*, **1**,
463 129–137.

464

465 **Figure captions**

466 Figure 1: In-field data acquisition in HCP geometry for the GEM-2 (Geophex Ltd.) on a
467 Neolithic magoules (credit: Meropi Manataki). Instrument is hold at a height of 0.3 m in a
468 hand operating acquisition mode.

469 Figure 2: Opposites of the responses, expressed by H_s/H_p ratio, (a) versus conductivity for κ_{ph}
470 $= 50 \cdot 10^{-5}$ S.I., and (b) versus in-phase susceptibility for $\sigma=50$ $\Omega \cdot m$ (the quadrature
471 susceptibility being 6% of the in-phase), at 5 kHz and 40 kHz for the GEM-2 instrument when
472 held at 0.3m height above ground surface.

473 Figure 3: In-phase (a) and quadrature response (b) as functions of the height above ground
474 surface, GEM-2, for $\kappa_{ph}=50 \cdot 10^{-5}$ S.I., and $f=5010$ Hz.

475 Figure 4: Quadrature response as functions of the quadrature out-of-phase part of the
476 magnetic susceptibility for both 100 and 500 $\Omega.m$ and $f=5010\text{Hz}$

477 Figure5 : (a) Apparent magnetic susceptibility and (b) apparent magnetic viscosity variations
478 with increasing the thickness of the first layer for 5010 Hz and 13370 Hz frequencies.

479 Figure 6: Value of the apparent magnetic viscosity obtained with the proposed procedure as a
480 function of electrical conductivity and magnetic viscosity a) $f=5010$ Hz and b) $f=13370$ Hz.

481 Figure 7: Result of the processing of synthetic data, a) simulated model, b) apparent electrical
482 conductivity, c) apparent magnetic susceptibility for 5010 Hz, d) apparent magnetic
483 susceptibility for 13370 Hz, e) apparent magnetic viscosity for 5010 Hz, f) apparent magnetic
484 viscosity for 13370 Hz.

485 Figure 8: Raw data for the site of Karatzantakli (Grece): a) In-phase measurement in ppm for
486 5010 Hz, b) In-phase measurement for 13370 Hz, c) Quadrature out-of-phase measurement
487 for 5010 Hz, d) Quadrature out-of-phase measurement for 13370 Hz.

488 Figure 9: Processed data for the site of Karatzantakli (Greece): a) apparent electrical
489 conductivity, b) apparent magnetic susceptibility for 5010 Hz, c) apparent magnetic
490 susceptibility for 13370 Hz, d) apparent magnetic viscosity for 5010 Hz, e) apparent magnetic
491 viscosity for 13370 Hz.

492 Figure 10: Raw data for the site of Almiriotiki (Greece): a) In-phase measurement in ppm for
493 5010 Hz, b) In-phase measurement for 13370 Hz, c) Quadrature out-of-phase measurement
494 for 5010 Hz, d) Quadrature out-of-phase measurement for 13370 Hz.

495 Figure 11: Processed data for the Neolithic site of Almiriotiki (Greece): a) apparent electrical
496 conductivity, b) apparent magnetic susceptibility for 5010 Hz, c) apparent magnetic

497 susceptibility for 13370 Hz, d) apparent magnetic viscosity for 5010 Hz, e) apparent magnetic
498 viscosity for 13370 Hz.

499

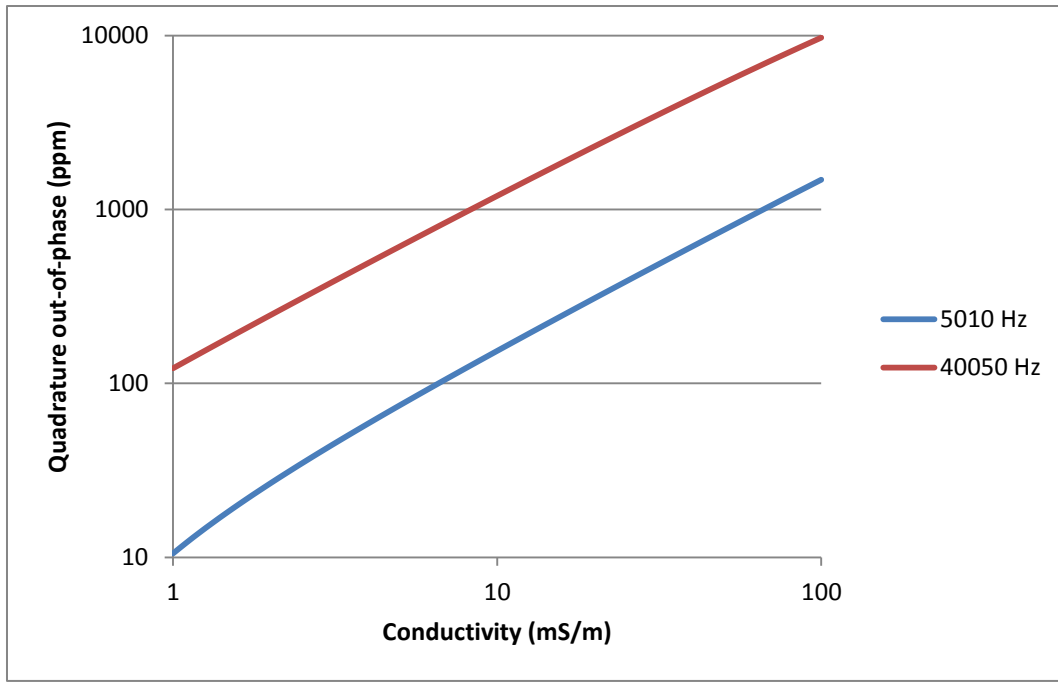


500

Fig. 1

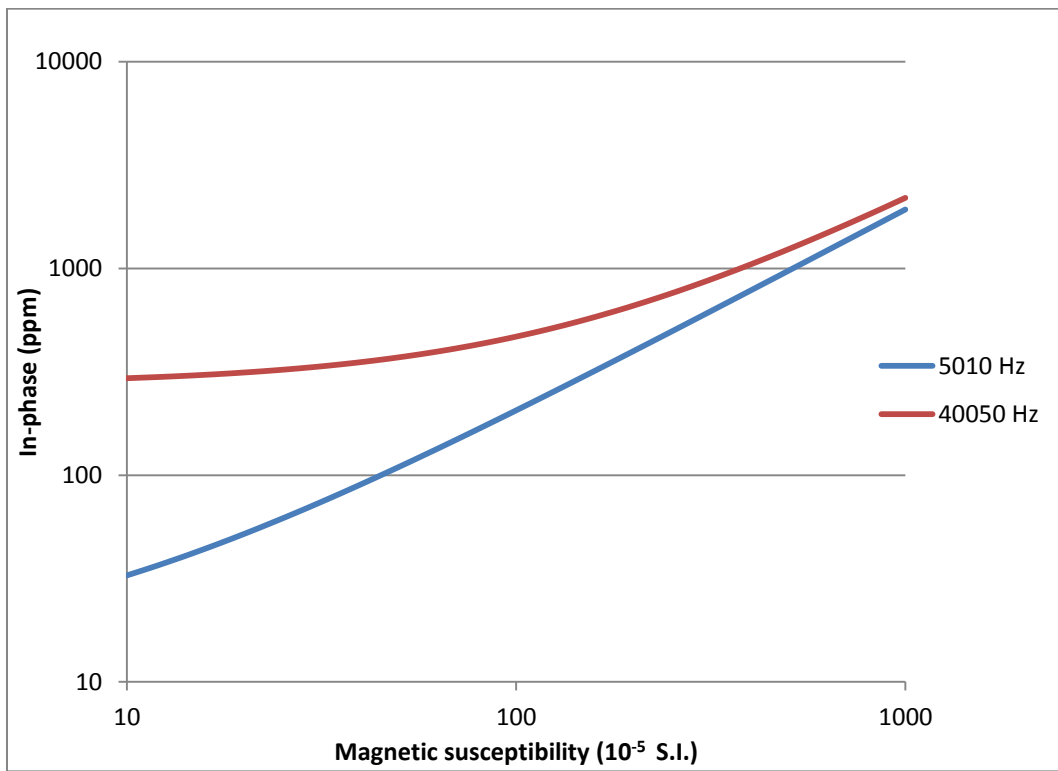
501

502



503

Fig. 2a

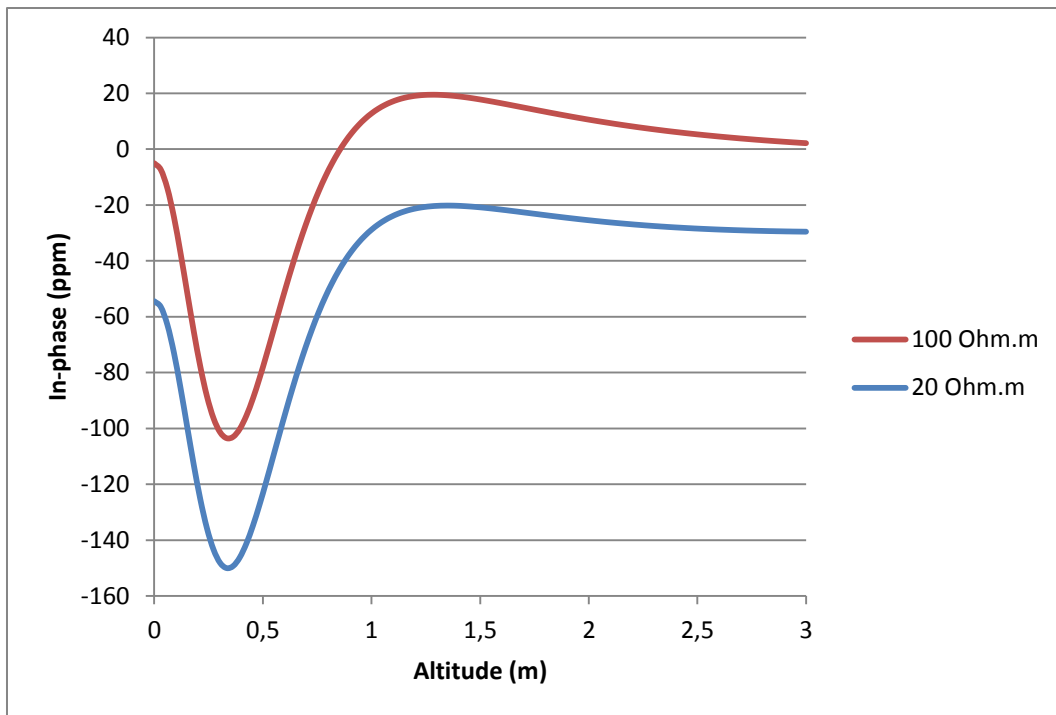


504

Fig. 2b

505

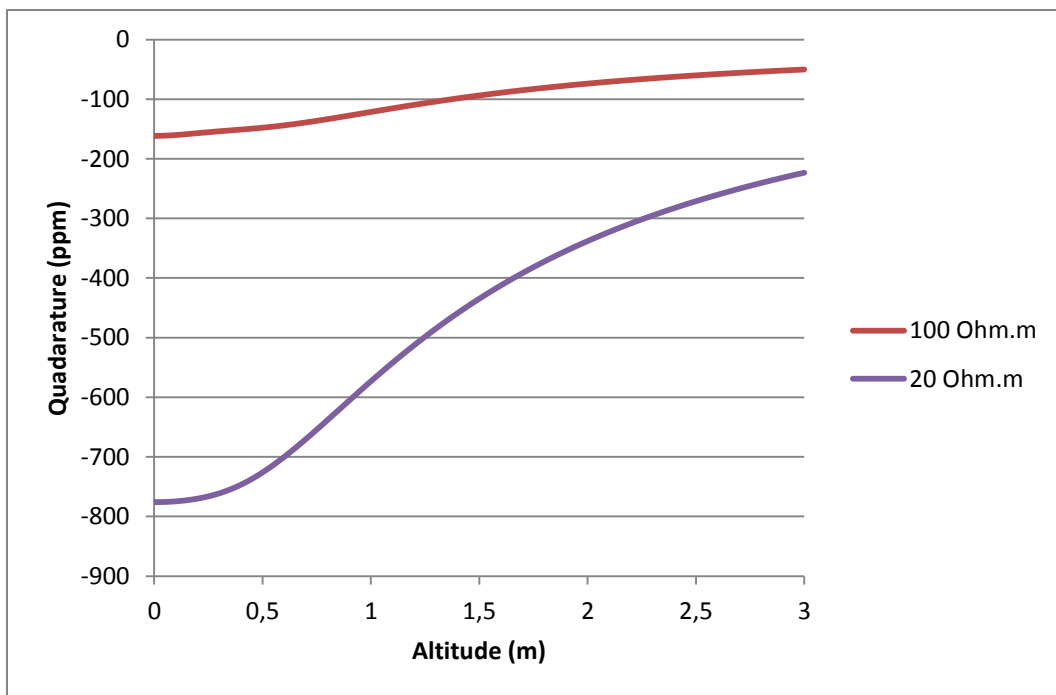
506



507

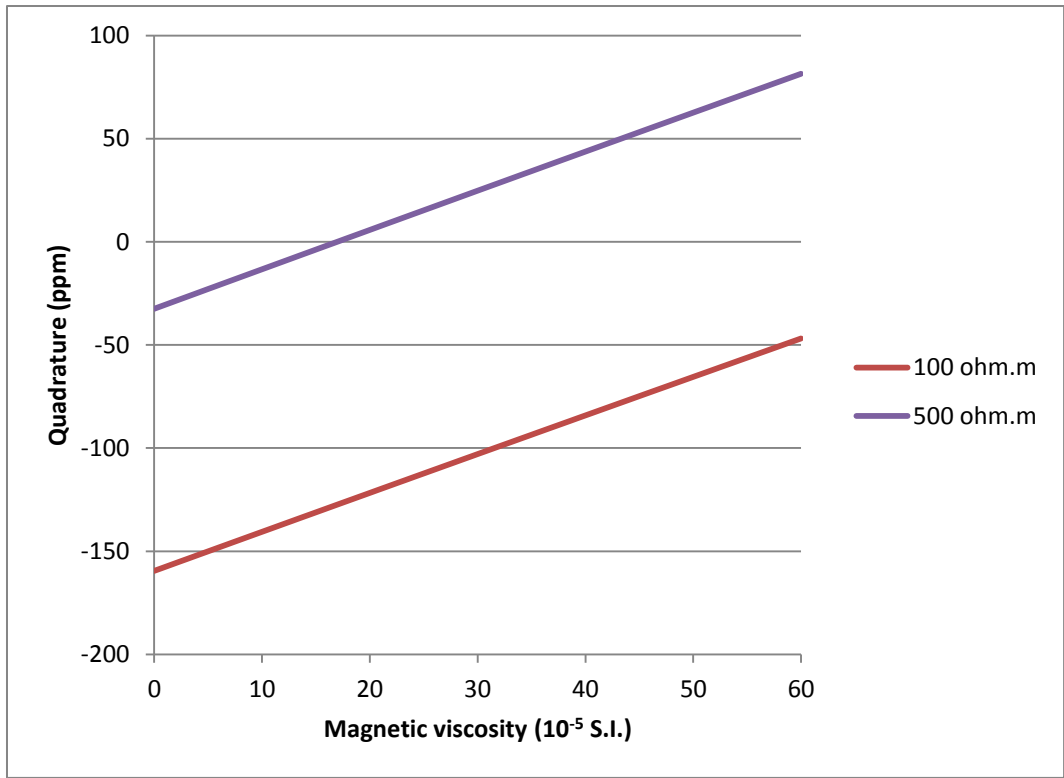
Fig. 3a

508



509

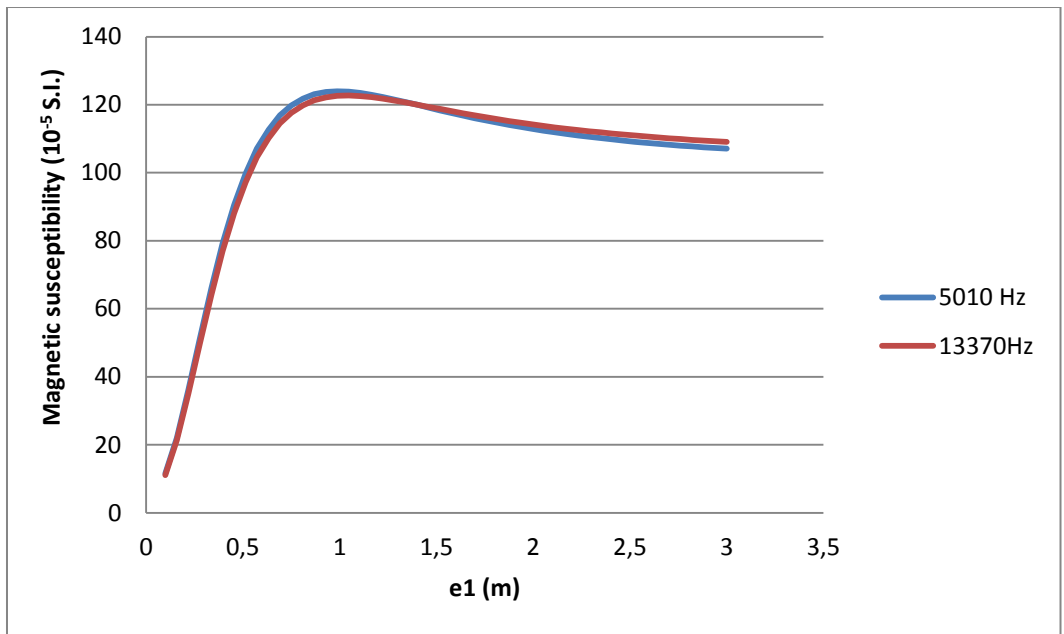
Fig. 3b



510

Fig. 4

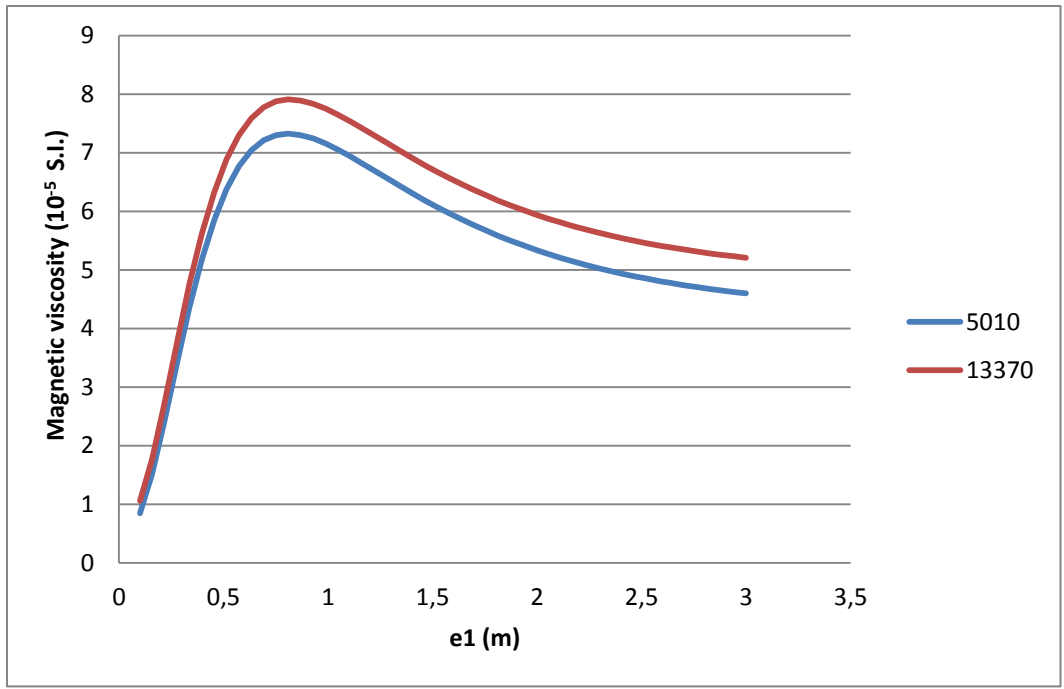
511



512

Fig. 5a

513



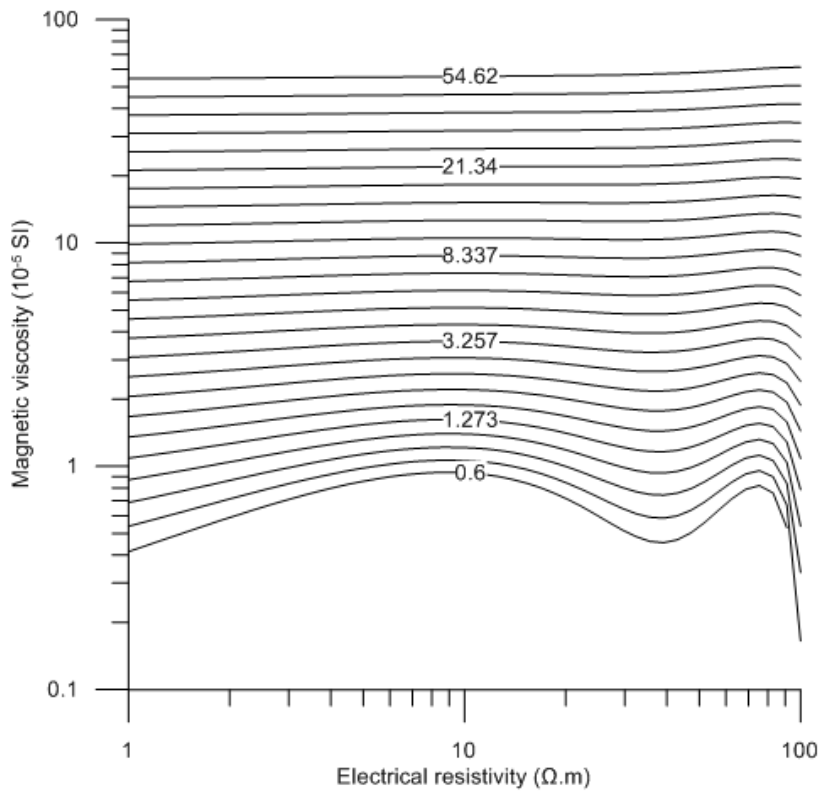
514

Fig. 5b

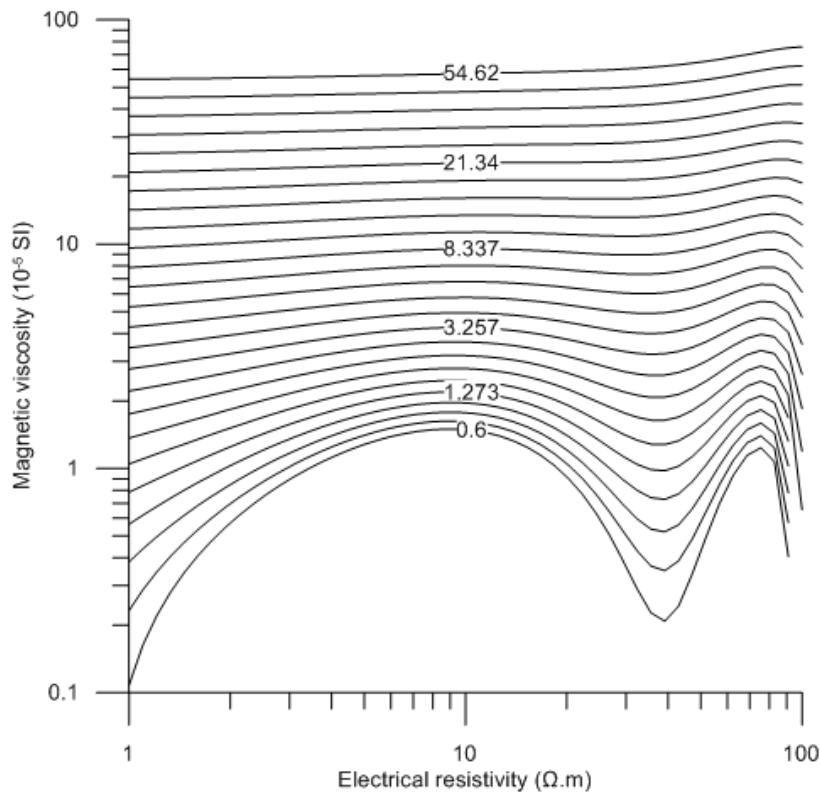
515

516

517



a. Value of the apparent magnetic viscosity obtained with the proposed procedure as function of electrical conductivity and magnetic viscosity $f=5010$ Hz



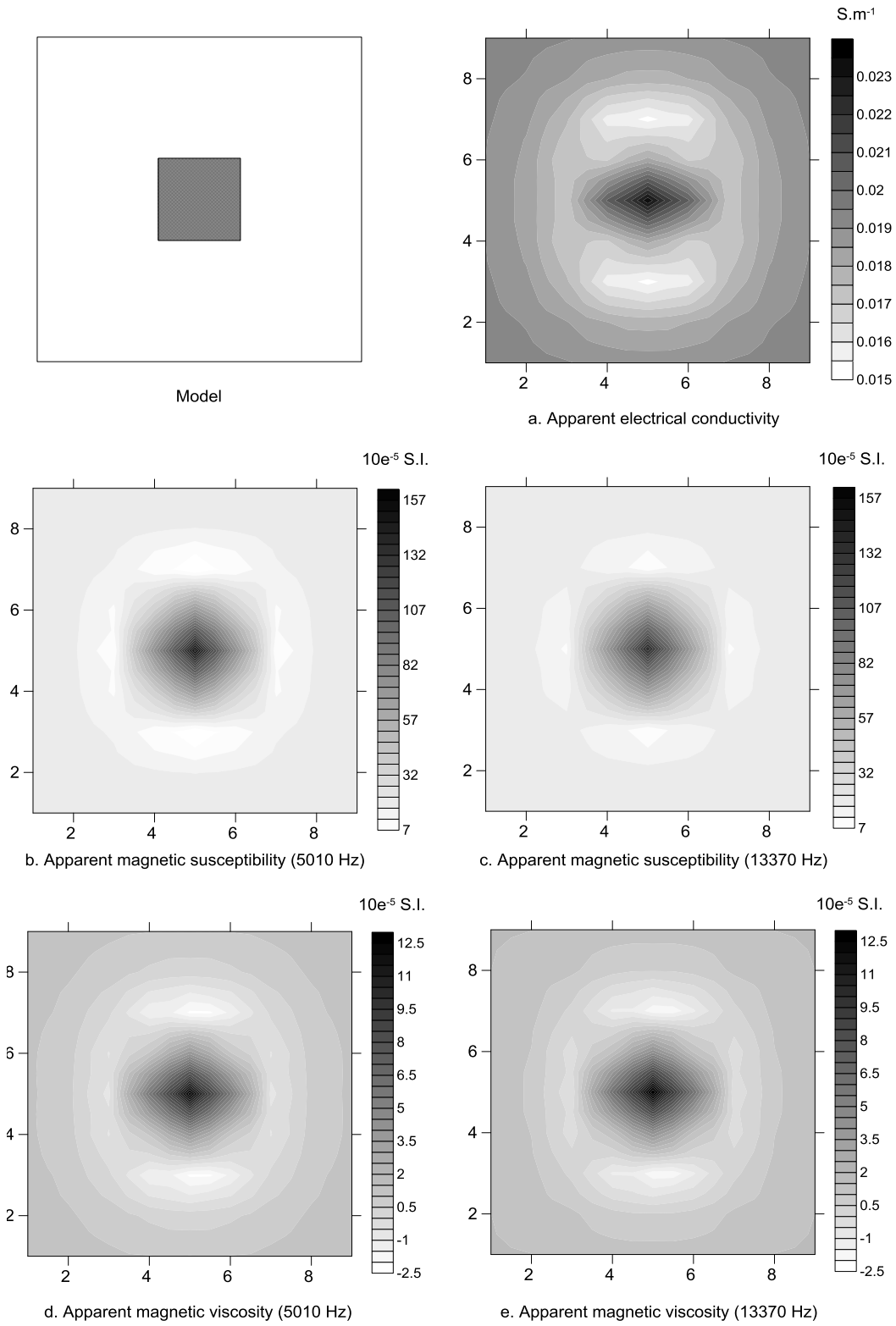
b. Value of the apparent magnetic viscosity obtained with the proposed procedure as function of electrical conductivity and magnetic viscosity at $f=13370$ Hz

518

519 Fig. 6

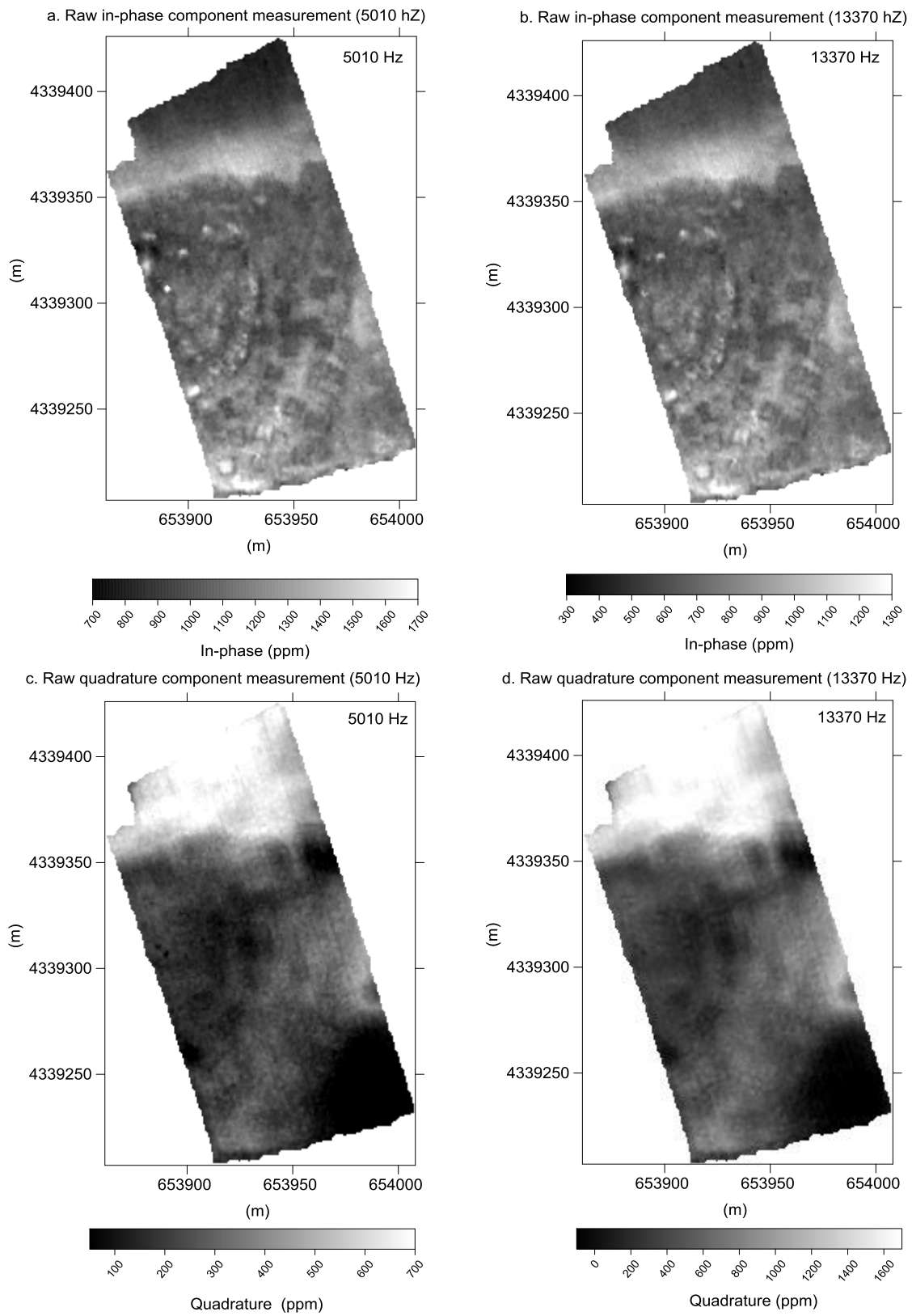
520

521



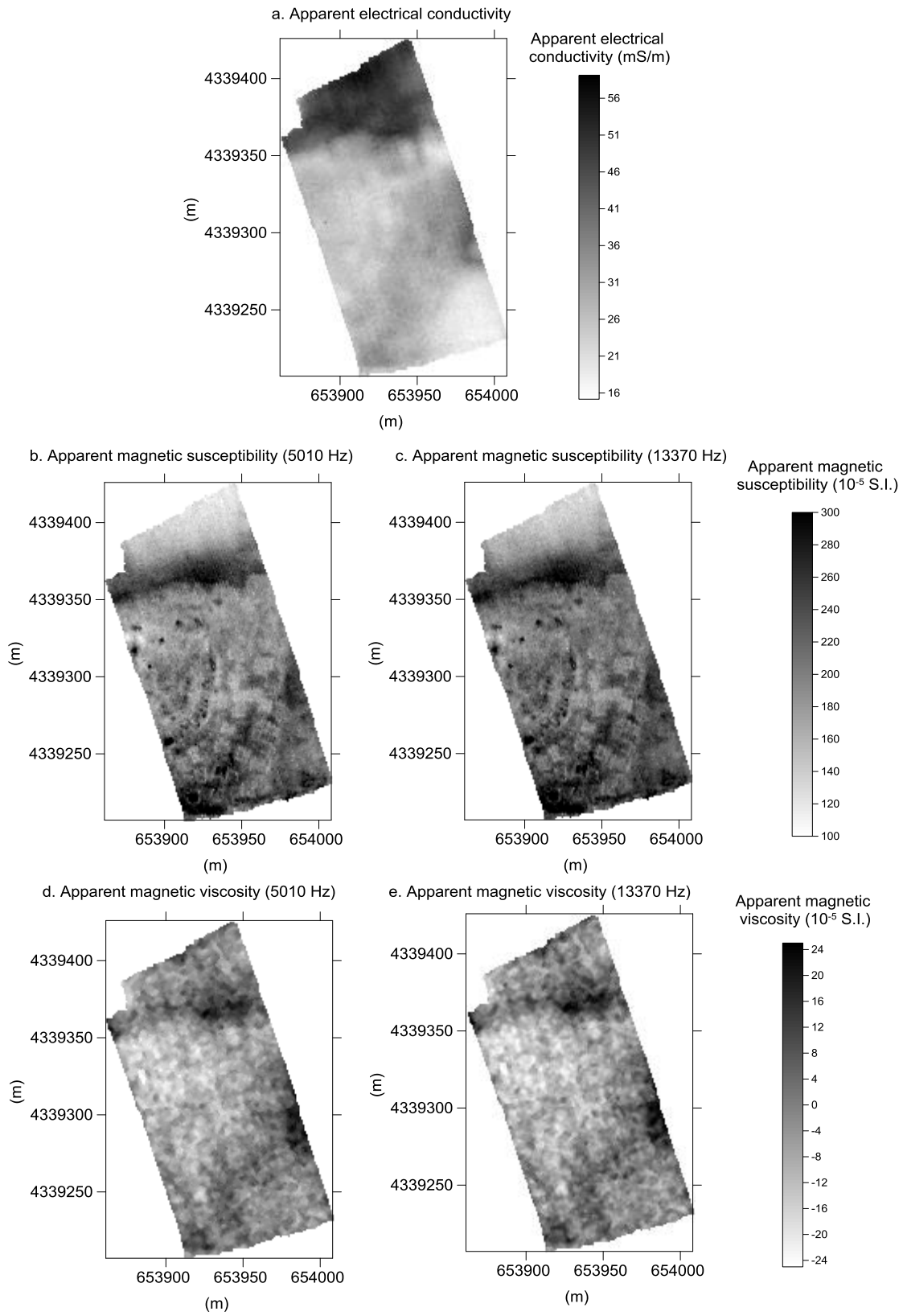
522

523 Figure 7



524

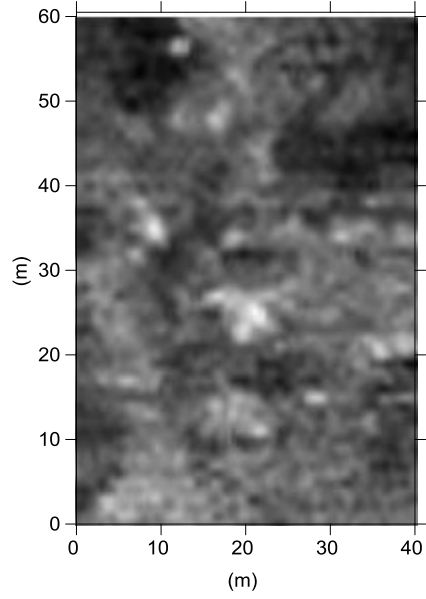
525 Fig. 8



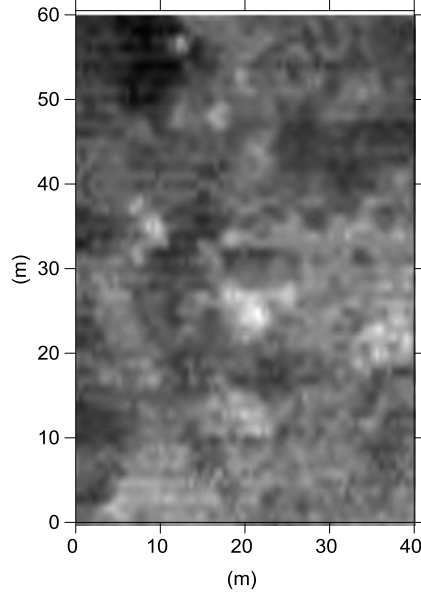
526

527 Fig. 9

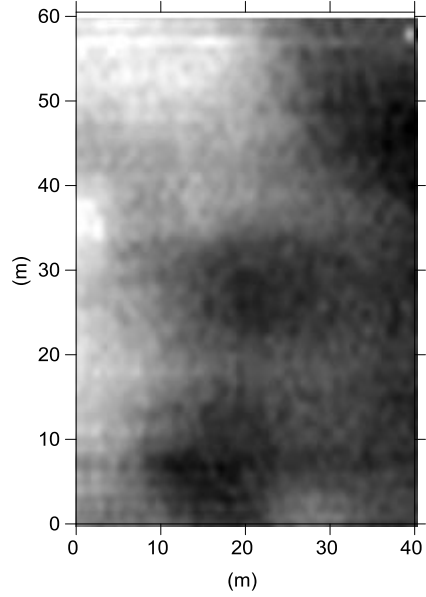
a. Raw in-phase component measurement (5010 hZ)



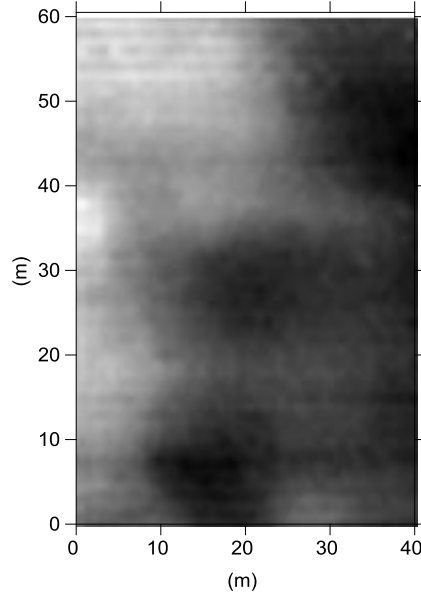
b. Raw in-phase component measurement (13370 hZ)



c. Raw quadrature component measurement (5010 hZ)

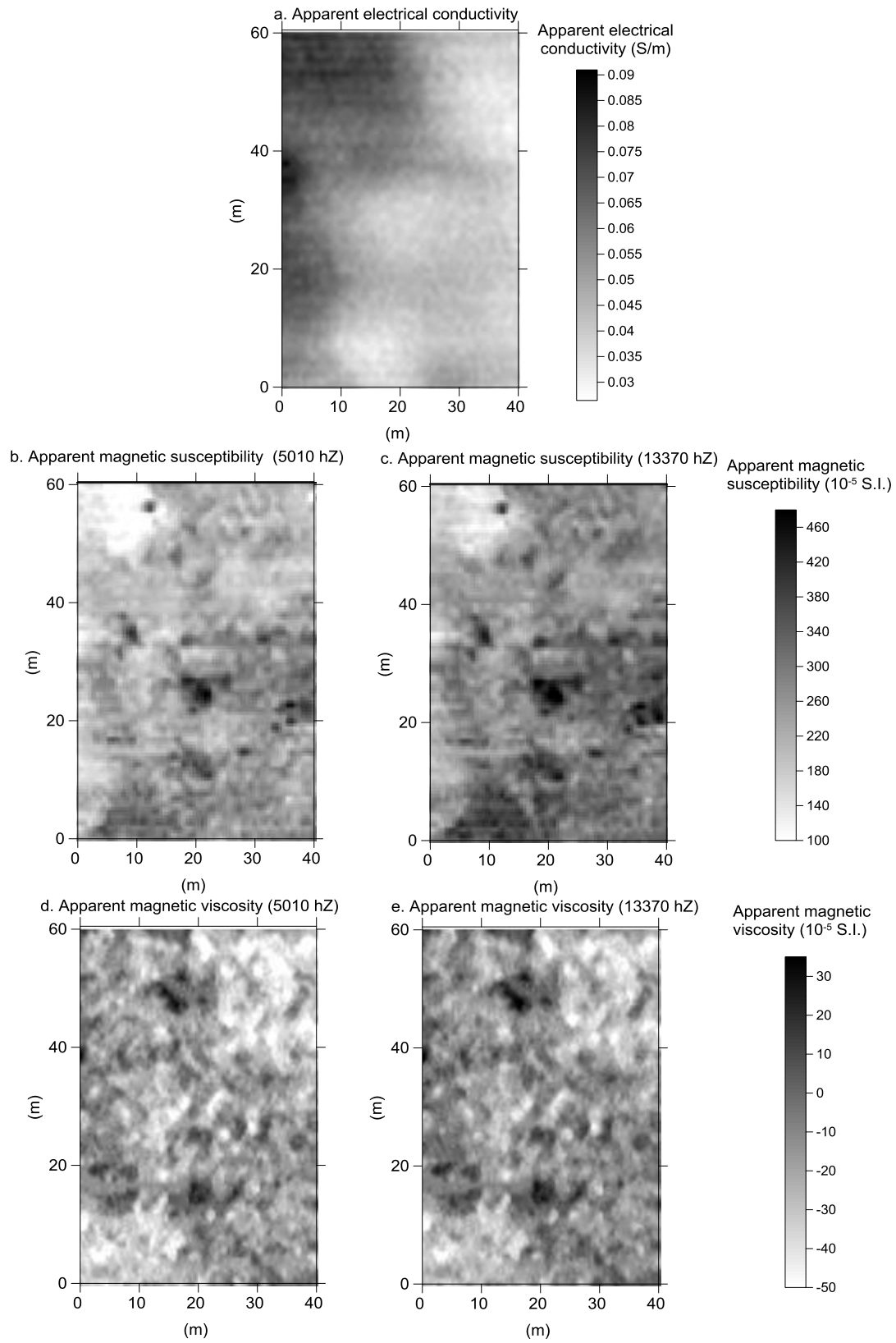


d. Raw quadrature component measurement (13370 hZ)



528

529 Fig. 10



530

531 Fig. 11

532